

L₁ SPIR-iT: Autocalibrating Parallel Imaging Compressed Sensing

M. Lustig¹, M. Alley², S. Vasanawala², D. L. Donoho³, and J. M. Pauly¹

¹Electrical Engineering, Stanford University, Stanford, CA, United States, ²Radiology, Stanford University, ³Statistics, Stanford University

Introduction: Parallel imaging (PI) [1,2] is a well-established acceleration technique based on the spatial sensitivity of array receivers. Compressed sensing (CS) [3-5] is an emerging acceleration technique that is based on the compressibility of medical images. Attempts to combine [8-13] the two have been limited to straightforward extensions of SENSE [2] with SparseMRI [5]. Here we present a detailed approach on synergistically combining auto-calibrating parallel imaging (acPI) [6,7] with CS. The acquisition and the reconstruction are carefully optimized to meet the requirements of both methods in order to achieve highly accelerated robust reconstructions.

Theory: A successful CS reconstruction requires (i) sparsity of representation, (ii) incoherent sampling, and (iii) non-linear sparsity enforcing reconstruction. Here, we reconsider these requirements in the context of acPI and propose: a modified sparsity model for multiple coil images, an incoherent sampling scheme that does not harm the conditioning of acPI reconstruction, and an acPI reconstruction scheme that uses both the coil and the sparsity information.

Methods: **I. Joint sparsity** of phased array images: The sparse transforms (here, wavelet) of the individual coil images are correlated; therefore we propose a joint sparsity functional [14] that takes the correlation into account. The usual definition of the L₁ norm with a single coil is $\sum_i |w(r)|$, or the sum of absolute values of all transform coefficients. We define the vector $w(r)=[w_1(r), \dots, w_n(r)]^T$ to be the coefficients at position r across all n coils, and generalize the L₁ norm to be the sum of magnitudes $\sum_i \|w(r)\|_2$. **II. Incoherent sampling:** Random sampling provides the high degree of incoherence needed for compressed sensing. However, it is not optimized for parallel imaging. Frequently occurring large gaps between samples reduce the reconstruction conditioning and increase noise. Sampling according to a (gridded) Poisson-disc distribution [15,16] provides high degree of incoherence and at the same time uniform distance between samples (See Figs. 1 and 2). It also provides flexibility for fractional and anisotropic acceleration (using ellipsoids rather than discs), resulting in a better fit to different coil array geometries (See Fig. 2). **III. Reconstruction:** We use an iterative GRAPPA-like approach that is described in detail in [7,17], which we refer to as SPIR-iT (iterative Self-consistent Parallel Imaging Reconstruction). It enforces self-consistency with the calibration and data acquisition. Here, in addition we enforce the sparsity of the reconstruction. We minimize the following constrained functional: minimize $\sum_i \|w(r)\|_2$ subject to: $Gx=x$, $x|_{\text{acq}}=y$, $w=\Psi F^{-1}x$, where x are the desired k-space data, y are acquired k-space points, F is a Fourier transform operator, Ψ is a sparse transform (wavelet), w are sparse transform coefficients, and G is a GRAPPA-like convolution operator similar to [7,17] that is obtained by calibration.

For simplicity, in this work the reconstruction is implemented as a projection over convex sets (POCS) algorithm. (i) Set $x_0=0$ (ii) Apply $x_{i+1}=Gx_i$ (iii) Set $x_{i+1}|_{\text{acq}}=y$ (iv) compute $w=\Psi F^{-1}x_{i+1}$ (v) set $w(r)=\text{SoftThresh}(\|w\|_2, \lambda)$ (vi) compute $x_{i+1}=F\Psi^{-1}w$ (vii) Set $x_{i+1}|_{\text{acq}}=y$ (viii) repeat till convergence. The soft-threshold operation is equivalent to L₁ penalty [18] and is defined as: $\text{SoftThresh}(w, \lambda) = w/\|w\|_1 \cdot \{\|w\|_1 - \lambda\}_+$. Alternatively, more advanced optimization methods (nl-Conjugate-gradient, Interior-point, etc.) can be applied.

Results: A patient with recurrent tumor in the lower extremities was scanned after administration of a contrast agent using a fat suppressed 3D SPGR sequence on a 1.5T GE Signa Excite scanner. The following parameters were used: TR/TE(partial echo) 4.27/1.14ms, matrix=256x320x106, FOV=32x32x21.2cm, flip=15°, acPI calibration=24x24 samples, coil array=4, sampling: Poisson-disc phase encodes, 2D acceleration=5 (2.5x2). The data was reconstructed with ARC (GE's acPI product reconstruction), CS-wavelet without parallel imaging (Matlab code) and L₁-wavelet SPIR-iT (Matlab code). The result in Fig. 3 shows the superior reconstruction of L₁ SPIR-iT.

Conclusions: We presented a method to combine CS and acPI. We optimized the sampling and the reconstruction such that the two techniques add synergistically. We demonstrated good robust diagnostic quality reconstruction at acceleration beyond the number of coils.

References: [1] Sodickson MRM 1997;38(4):591-603 [2] Pruessmann MRM 1999;42(5):952-962 [3] Cande's et al., IEEE TIT 2006;52(2):489-509 [4] Donoho, IEEE TIT 2006;52(4):1289-306 [5] Lustig et. al MRM 2007;58(6):1182-95 [6] Griswold et. al MRM 2002;47(6):1202-10 [7] Lustig et. al ISMRM'07 [8] King et. al ISMRM'08 [9] Bing et. al ISMRM'08 [10] Zhao et. al ISMRM'08 [11] Marinelli et. al ISMRM'08 [12] Uecker et. al ISMRM'08 [13] Liu et. al ISMRM'08 [14] Tropp et al., ICASSP 2005 [15] Dunbar et. al SIGGRAPH'06 [16] Nayak et. al ISMRM'98 [17] M. Lustig, PhD Thesis, Stanford University [18] Johnstone et. al Biometrika, 1994;81:425-455

Figure 3: 5-fold (2.5x2), 4-coils, 2D Poisson-disc accelerated, post contrast lower extremity axial and coronal slices showing enhanced lesions (arrows) and vessels. Left: ARC reconstruction (GE's acPI product) showing significant (incoherent) noise artifacts. Middle: CS reconstruction showing reduced artifacts, but some loss of contrast, subtle features and resolution. Right: L₁ SPIR-iT reconstruction, which combines auto-calibrating parallel imaging with compressed sensing, shows reduced noise artifacts with better depiction of subtle features and resolution.

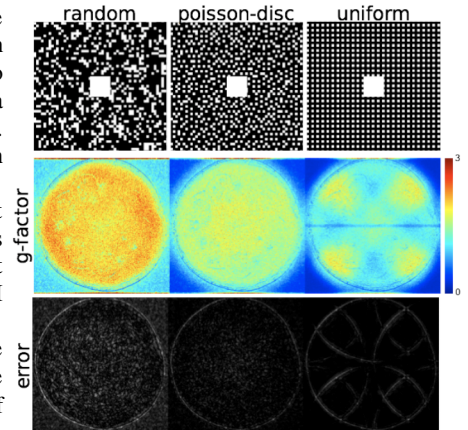


Figure 1: g-factor and error maps obtained from a 100 scans. Top: Poisson-disc sampling is both incoherent and uniformly distributed in k-space. Middle (in color): The noise amplification in Poisson-disc sampling is significantly smaller than random sampling and of the order of uniform sampling. Bottom: The residual error in Poisson-disc sampling is incoherent as opposed to coherent residual in uniform sampling

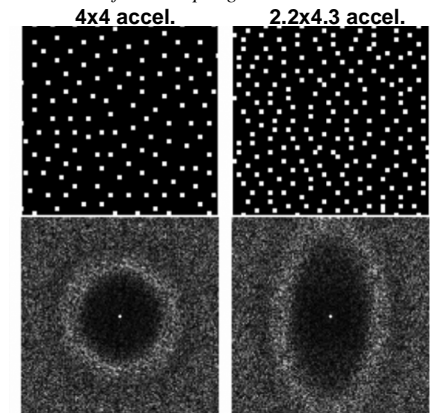


Figure 2: An example of a 4x4 and a 2.2x4.3 2D accelerated Poisson disc sampling patterns and their associated point spread functions. The incoherent aliasing appears beyond the Nyquist-rate supported field of view. Non-isotropic FOV can be used to adapt to coil array geometries.

